Passive Thermal Compensation of the Optical Bench of the Galaxy Evolution Explorer

Virginia Ford*[a]
Rick Parks[b]
Michelle Coleman[a]

ABSTRACT

The Galaxy Evolution Explorer is an orbiting space telescope that will collect information on star formation by observing galaxies and stars in ultraviolet wavelengths. The optical bench supporting detectors and related optical components used an interesting and unusual passive thermal compensation technique to accommodate thermally-induced focal length changes in the optical system. The proposed paper will describe the optical bench thermal compensation design including concept, analysis, assembly and testing results.

Keywords: Ultraviolet, passive athermalization, space telescope, optomechanical design

1. INTRODUCTION

The Galaxy Evolution Explorer (GALEX) is a small Explorer mission that is part of NASA's Structure and Evolution of the Universe Theme. It was launched on the 23rd of April 2003 on a Pegasus rocket and is orbiting Earth and observing galaxies in the ultraviolet waveband.

Its science goals include: survey the sky to produce a comprehensive ultraviolet map of the galaxies forming in the nearby Universe; learn about the galaxy forming regions, what chemical elements are present, and gain understanding of the processes that formed our Milky Way galaxy; compare ultraviolet data with data in other wavebands to gain greater understanding of the processes involved in galaxy formation; and identify intriguing celestial objects for study by other telescopes. Figure 1 shows a composite data picture produced in June 2003 of Galaxy Centaurus A with combined images from GALEX (UV - blue and green) and Chandra (X-ray - red) demonstrating how multiple waveband enhance understanding of galaxy formation. Figure 2 shows a picture taken by GALEX of Galaxy NGC 300 taken by GALEX in ultraviolet light. Bright blue regions in the image indicate the formation of new stars.

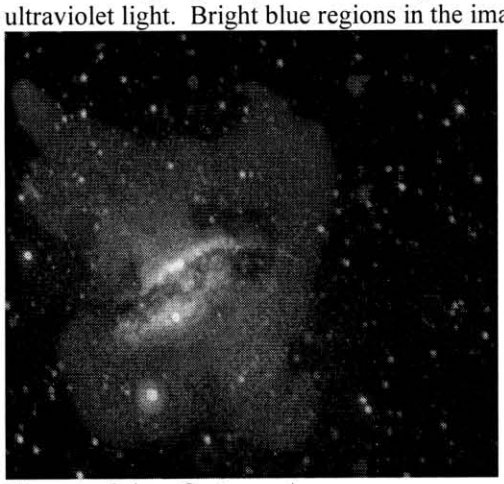

Figure 1. Galaxy Centaurus A

Figure 2. Galaxy NGC 300[1]

* Virginia.g.ford@jpl.nasa.gov; phone 810-354-0048; Jet Propulsion Laboratory
a. Jet Propulsion Laboratory
b. Acro Service Corporation

2. DESIGN DESCRIPTION

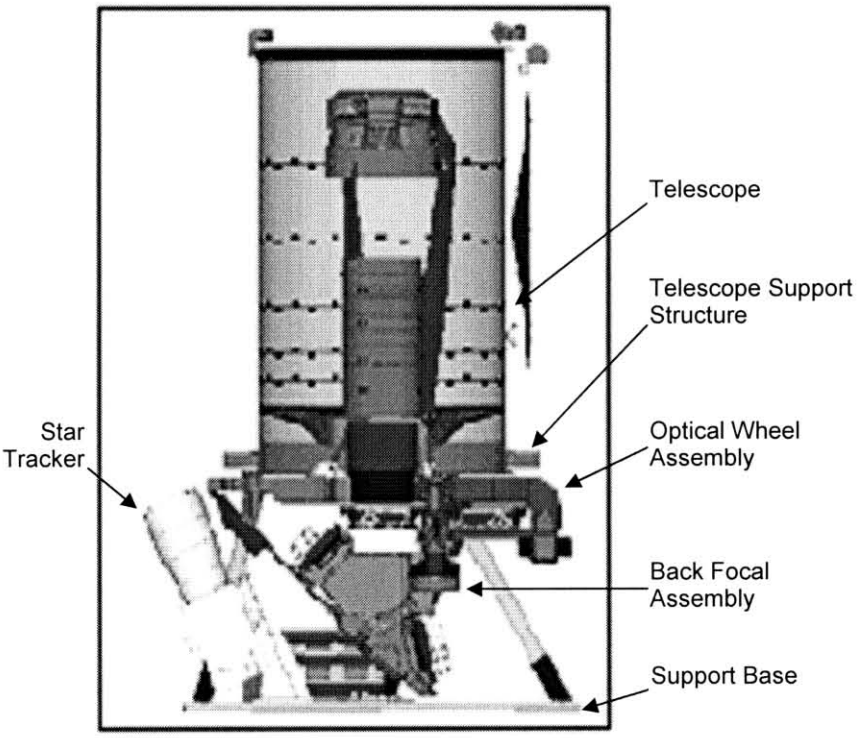

Figure 3. The payload assembly of GALEX

The GALEX payload consists of three major subsystems: Telescope, Back Focal Assembly, and an Optical Wheel Assembly. They are integrated together on a single structure called the Telescope Support Plate. The Telescope Support Plate (TSP) is then mounted to a Support Base holding the electronics and a Star Tracker that interfaces to the spacecraft. Figure 3 shows the payload assembly.

The telescope consists of an obscured on-axis primary and secondary assembly with the secondary mirror supported on a composite spider that is supported from a hub mounted to the center of the primary mirror. The primary mirror is supported from its central hub through three bipods to the Telescope Support Plate. Figure 4 shows the telescope subsystem.

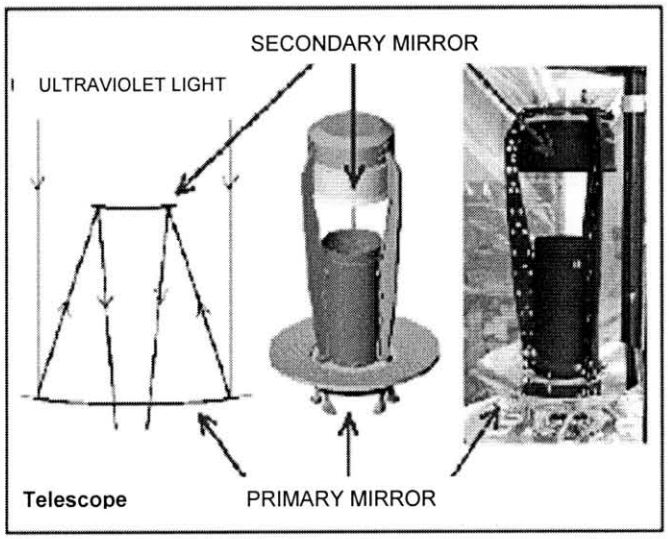

Figure 4. GALEX Telescope subassembly

The Optical Wheel Assembly shown in Figure 5 rotates either a Grism or a compensating window into the field of view. The Grism consists of a prism with a diffraction grating that splits the light into wavebands for spectral data collection. The mechanism consists of a rotating plate that carries both optical components. The Optical Wheel Assembly attaches directly to the Telescope Support Plate.

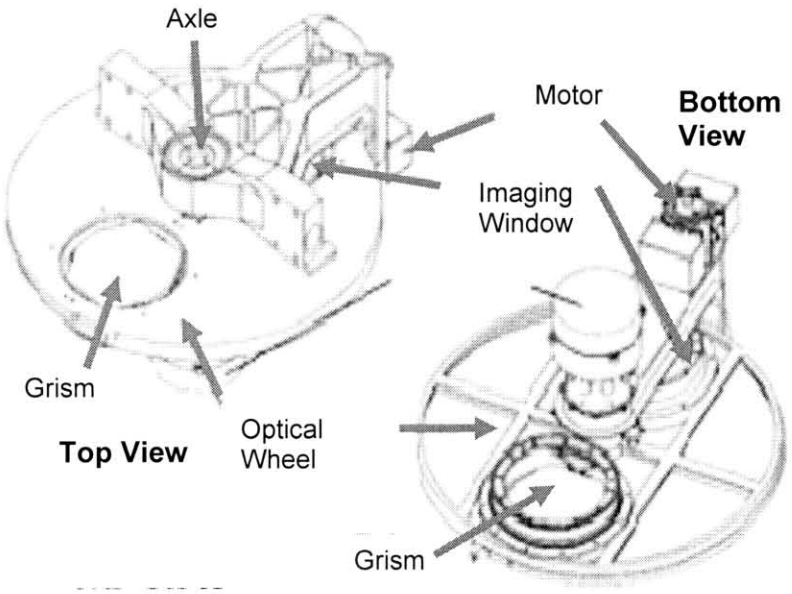

Figure 5. Optical Wheel Assembly

The Back Focal Assembly consists of the optical and electro-optical components shown in Figure 6. The optical beam from the telescope enters the Back Focal Assembly after it has passed through the Optical Wheel Assembly. The beam encounters a slightly aspheric dichroic beam splitter which reflects the far ultraviolet light towards the far ultraviolet detector (FUV) and transmits the near ultraviolet light towards a flat mirror and into the near ultraviolet detector. The focus of this talk will be the passive athermalization concept used for the Back Focal Assembly.

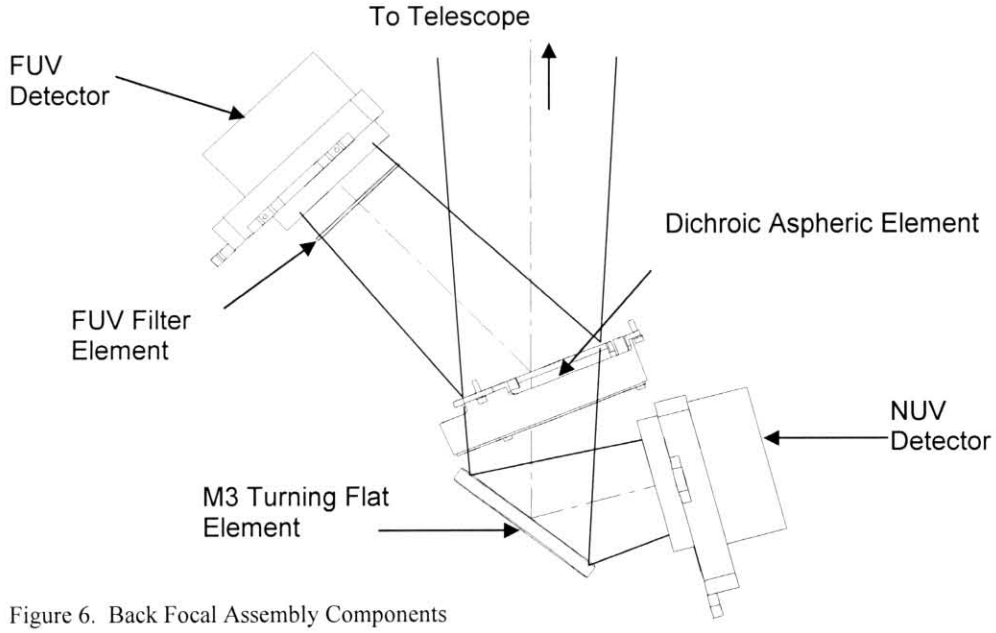

Figure 6. Back Focal Assembly Components

A view of the Back Focal Assembly optomechanical structures is shown in Figure 7. In addition to the optical components, the assembly consists of three symmetrical bipods made of Invar and a two part aluminum optical bench.

The Invar bipods mount to the Telescope Support Plate. These structures passively position the optical components including the two detectors so that they stay within the required focal range as the system changes temperature

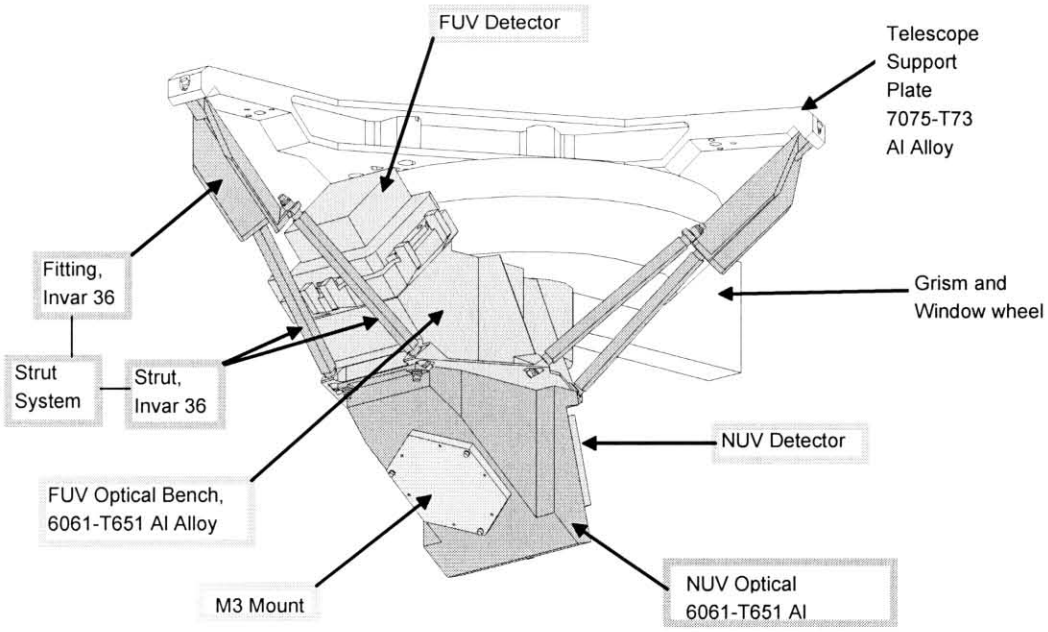

Figure 7. Back Focal Assembly

3. BACK FOCAL ASSEMBLY PASSIVE ATHERMALIZATION CONCEPT

The thermal requirement for the optics of GALEX were that the telescope operate between -15C to +25C, the Back Focal Assembly (BFA) optics operate at -15C to +25C, the Detector windows operate at -10C to +30C and the Detector Focal Planes work at 0C to +30C. Initial temperature predictions are shown in Table 1, with all components falling within their required ranges during both hottest case during an orbit and coldest case during an orbit. The system was required to stay in focus from room temperature alignment to flight operational temperatures

Table 1. Predicted Hot Case and Cold Case Temperatures

Subassembly	Number	Cold Case (°C)	Hot Case (°C)
Telescope Support Plate	22	-9.3 to -10.0	8.0 to 9.1
Strut System	24	-7.0 to -3.2	11.8 to 15.7
Optical Bench	26-32	-0.1 to 4.2	18.8 to 24.0
NUV Detector	33	5.8	24.9
FUV Detector	34	3.9	22.3
M3	35	2.6	23
Dichroic	28	2.4	21.9

Originally, the entire payload, both the Telescope and Back Focal Assembly (BFA), were athermalized together. The assembly of BFA opto-mechanical parts was able to move enough to accommodate the shift in focus delivered by the telescope as well as the change in location of the detectors. The decrease in temperature of the system from the position of original room temperature alignment required the BFA to move away from the telescope. By choosing to fabricate the TSP out of aluminum, the Optical Bench out of Titanium, and the struts out of stainless steel, when temperature decreased, the radius of attachment of the struts on the optical bench decreased, the radius of attachment of the struts on the TSP relatively increased, and the struts rotated to position the BFA correctly – with the stainless steel allowing the BFA to reach the correct focal position within 7μm for the NUV detector and within less than 1μm for the FUV detector. The conceptual design was developed using an excel spreadsheet based on the thermal equation

$$\Delta Z = \Delta T * L * CTE \quad (1)$$

and on trigonometric relationships of the bipod system. A copy of the excel spreadsheet is shown in Table 2.

Table 2. Method of estimating the capability of the bipod system during the conceptual design phase.

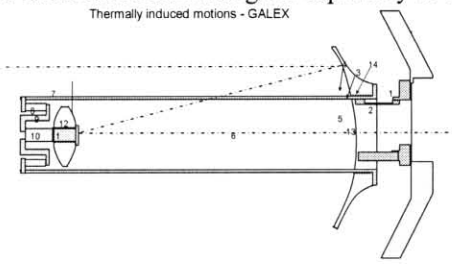

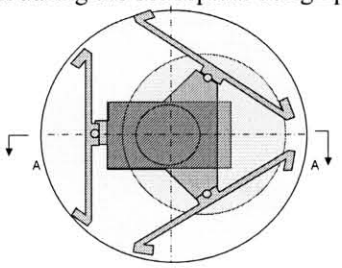

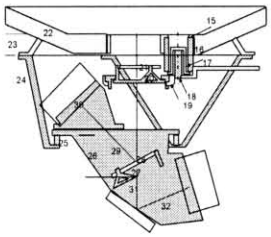

path #		optic mtl	th following mm	struc mtl	asumd ΔT	Δlen(z)		Δz	
1	interface plane		-15	ti	-40	0.006264		between	
2	flexure		-73.9	ti	-40	0.03087		intfc &	
3	flex to bondline cen		10.15	invar	-40	-0.0005278		primary	
4	bdln to edg of hole		-48.25	fused sil	-40	0.000579		0.0371403	
5	primary	glass	4.06359	fused sil	-40	-4.87631E-05		(smaller)	
5	pri vertx to edghol		-4.06359	fused sil	-40	4.87631E-05			
4	edghol to bdln cen		48.25	fused sil	-40	-0.000579		between	
4	bdln cen to edghol		-48.25	invar	-40	0.002509		primary &	
5	edghol to pri vertx		4.06359	invar	-40	-0.000211307		secondary	
6	to sec vertex		-610.2	invar	-40	0.0317304		-0.035932	
7	beyond sec		-62.5	invar	-40	0.00325		(smaller)	
8	al cyl		38	aluminum	-40	-0.036936			
9	inv cyl		-38	invar	-40	0.001976			
10	al cyl		38	aluminum	-40	-0.036936			
11	inv rod		12.25	invar	-40	-0.000637			
12	secondary	glass	12.25	fused sil	-40	-0.000147			
12	secondary	glass	-12.25	fused sil	-40	0.000147			
11	inv rod		-12.25	invar	-40	0.000637			
10	al cyl		-38	aluminum	-40	0.036936		between	
9	inv cyl		38	invar	-40	-0.001976		secondary &	
10	al cyl		-38	aluminum	-40	0.036936		intfc plane	
9	to sec vertex		62.5	invar	-40	-0.00325		-0.00142	
6	to prim vtx		610.2	invar	-40	-0.0317304		(smaller)	
13	to hub should		96.5	invar	-40	-0.005018			
14	should to bndln cen		-48.25	invar	-40	0.002509			
3	bndln cen to flex		-10.15	invar	-40	0.0005278		telescope sum	
2	flexure len		73.9	ti	-40	-0.03087		-0.00021	
1	flexure to intfc pl		15	ti	-40	-0.006264			
15			5	aluminum	-40	-0.00486			
16			62.5	ti	-40	-0.0261			
17			0	aluminum	-40	0			
18			0	ti	-40	0		between	
19			0	aluminum	-40	0		intfc plane	
20	grism struc	ti	5.5	ti	-40	-0.0022968		& grism	grism wheel sum
21	grism	glass	-6	CaF2UV	-40	0.004524	grism	-0.028733	-0.02873
22	backwd from intfc pln		0	aluminum	-40	0			
23	to bipod start		231.8	aluminum	-40	-0.2253096			
24	axial len bipods		85.00	cres	-40	0.288			
25	compens		0.00	ti	-40	0		between	
26	struct to dic flexmt		-9.302444	ti	-40	0.003884701		grism &	
27	dichroic flex		23.500	mixed	-40	0.00982		asphere	
28	asphere dichroic		4	suprasil	-40	-0.0000816	asphere	0.10455	
	reflective system							between	
29			183.1292	ti	-40	-0.076474754		asphere &	
30	det window		6	MgF2UV	-40	-0.005832		fuvdetector	fuv detector sum
	hdetector		5	steel	-30	-0.002595		-0.07587	-0.00005
	transmissive system								
27	dichroic flex		23.500	mixed		0.00982			
28	asphere	suprasil	4	suprasil	-40	-0.0000816			
31	reflector		81	ti	-40	-0.0338256		between	
32			105.2808	ti	-40	-0.043965262		asphere &	
	det window		6	suprasil	-30	-0.0000918	det window	nuvdetector	nuv detector sum
	detector			steel				-0.06885	0.00697

-0.00014

	CTE invar	1.30E-06
	CTE Ti	1.04E-05
	CTE al6061	2.43E-05
	CTE CaF2	1.89E-05
	CTE MgF2	2.43E-05
	CTE steel	1.73E-05
	CTE supras	5.10E-07
	CTE gr-cy	-1.06E-06
	CTE mag	2.52E-05
	CTE fus sil	3.00E-07
	CTEal4000	1.93E-05

-0.00005 -0.0001403

ΔT	lengths						ϕ	θ	New lengths						
	$radius_{ab}$	$radius_{th}$	$length_{bipod}$	len_{bipda}	len_{bpdr}	len_{bpdt}			$Nradius_{ab}$	$Nradius_{bp}$	$Nlength_{bpd}$	$Nlen_{bpdr}$	$Nlenbpd_t$	$Nlen_{bpda}$	Δlen_{bpda}
(°C)	(mm)(Ti)	(mm)(Al)	(mm)(Ti)	(mm)	(mm)	(mm)	(degrees)	(degrees)	(mm)	(mm)	(mm)	(mm)	(mm)	(mm)	(mm)
	Ti	Al	steel			OB support bipod									
-40	135	350.0	317.3326	85.000	40.000	303.109	74.3	25.201124	134.944	349.660	317.114	39.9	302.814	85.288	0.28821
	suprasil	Ti	Ti			Dichroic flexure analysis									
-40	55	63.226	39.0485	23.500	0.000	31.186	53.0	0	54.999	63.200	39.032	-0.022	31.173	23.490	-0.00982
	invar	ti	ti			telescope support									
-40	121	121.0	73.9000	73.900	0.000	0.000	0.0	0	120.994	120.949	73.869	0.0	0.000	73.869	-0.03087

After the feasibility of the concept was established via the spreadsheet, the final flight design was developed and the thermal performance was verified using thermal and structural finite element analysis. During this time, the requirements were changed so that the telescope subsystem was to be athermalized independently of the BFA using heaters. This programmatic choice enabled a more defined specification of the performance of the telescope subsystem

(developed by an independent vendor) and simplified the performance requirements on the BFA. The required motions of the BFA were reduced significantly which dictated a change in materials of the optomechanical structures to those listed in Figure 7. The flexible geometry of the BFA athermalization concept is shown in more detail in Figure 8.

Figure 8. BFA Athermalization system using 6 variables: the radius of attachment of the struts on the Telescope Support Plate (TSP),R; the radius of attachment of the struts on the optical bench,r; the length of the struts, and the materials of the TSP, the optical bench and the struts.

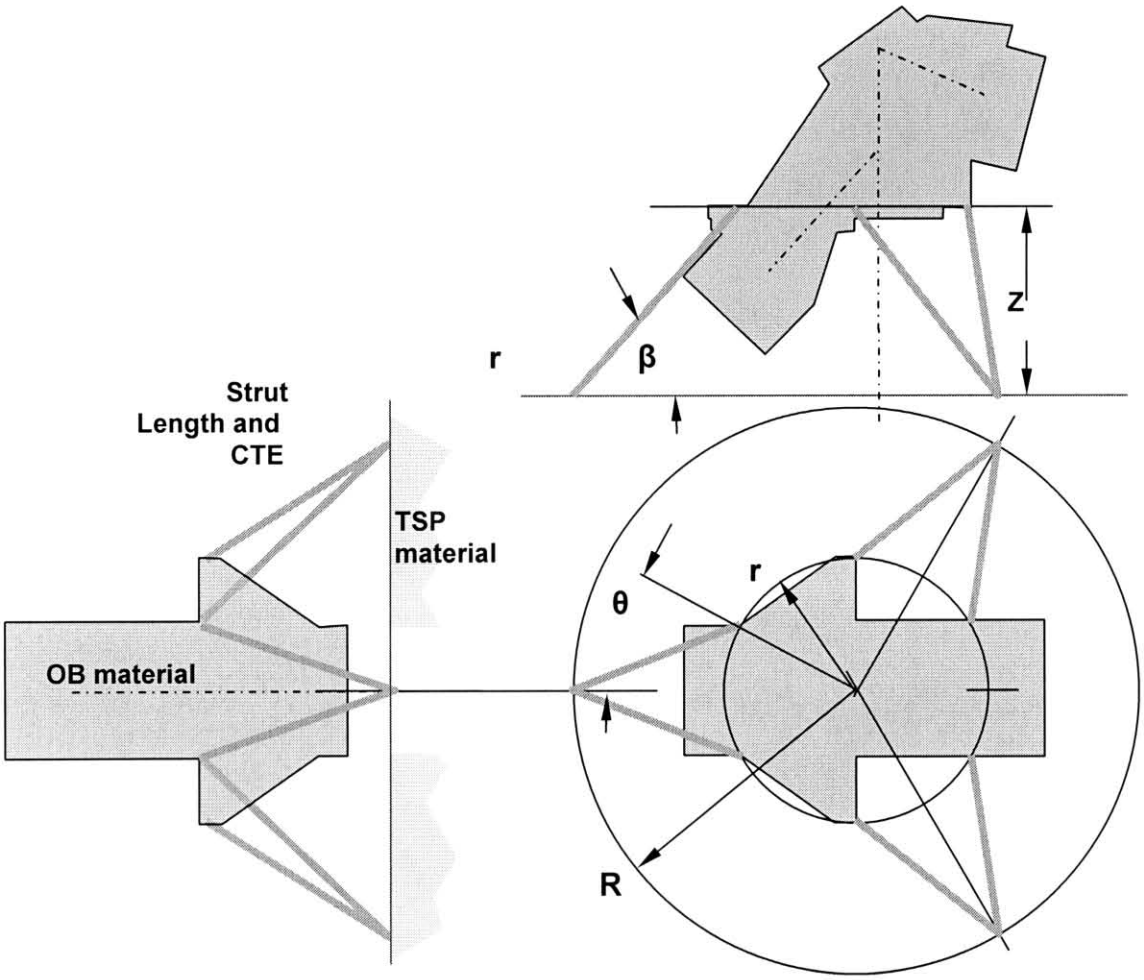

This athermalization system has 6 varible parameters – R, the radius of strut attachment to the TSP; r, the radius of strut attachment to the BFA; the length of the struts, and the materials of the TSP, the BFA, and the struts. This created a very sensitive and flexible athermalization system that enabled adaptation to changing requirements with small impact on design schedule. It features a strut geometry and material choices that can be tailored to create the change in focus length z with temperature that was required for optical performance of the Back Focal Assembly. As temperature changes, R, r, strut length and angle β change, moving the focus length z the required amount. The variety of variables enabled an inexpensive, workable design that considered on-orbit thermal environment predictions. The bipods consisted of three identical bipods, spherical washers both ends, with symmetric attachment to the Telescope Support Plate structure.

4. PERFORMANCE SENSITIVITY OF ATHERMALIZATION CONCEPT

The sensitivity of this design to changes in properties of the materials and lengths is illustrated in Figures 9, 10 and 11. Figure 9 shows a graph of the change in focal distance z with variation of R, the radius of attachment of the struts to the

TSP. As R varies in length as shown, the angle β increases from approximately 50 degrees to 90 degrees and slightly beyond. At the 90 degree position, the thermal performance of the system becomes identical to the performance of the invar alone – as if the BFA were supported on an invar collar. As the angle β becomes smaller, expansion of R and r create more motion causing a mechanical advantage that can be designed to meet the required performance.

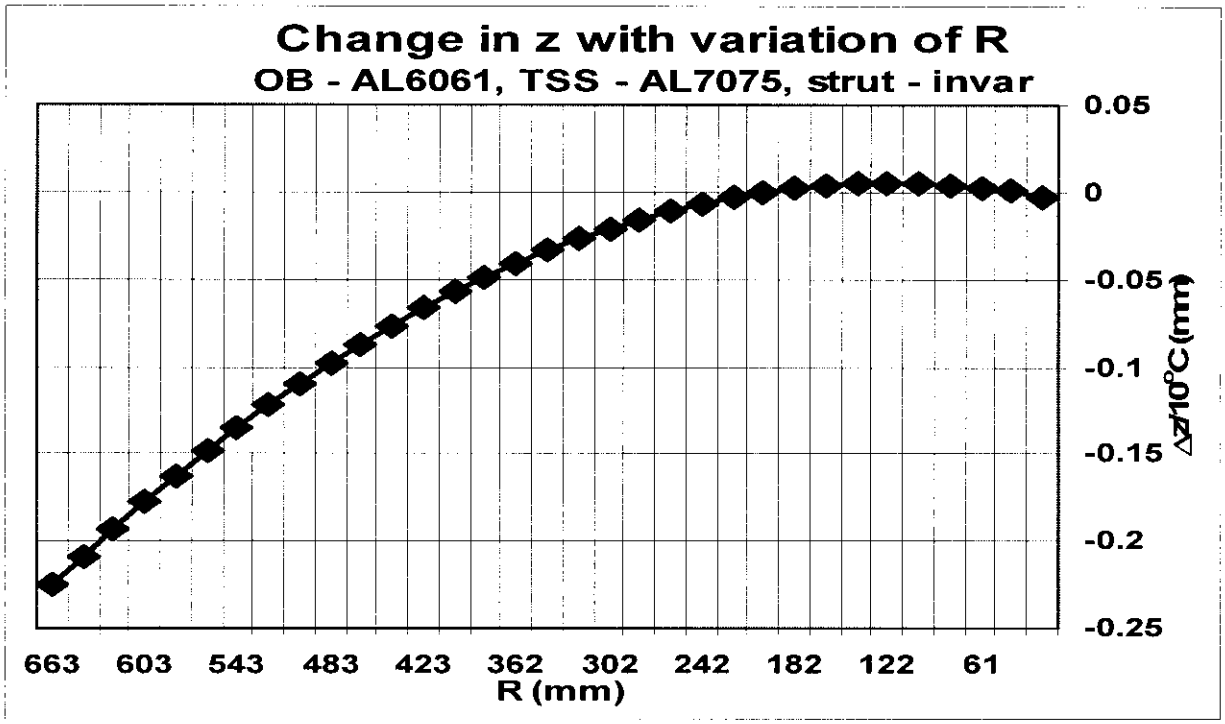

Figure 9. Change in z per 10°C versus variation of length R

Figure 10. Change in z per 10°C versus variation in BFA Optical Bench material

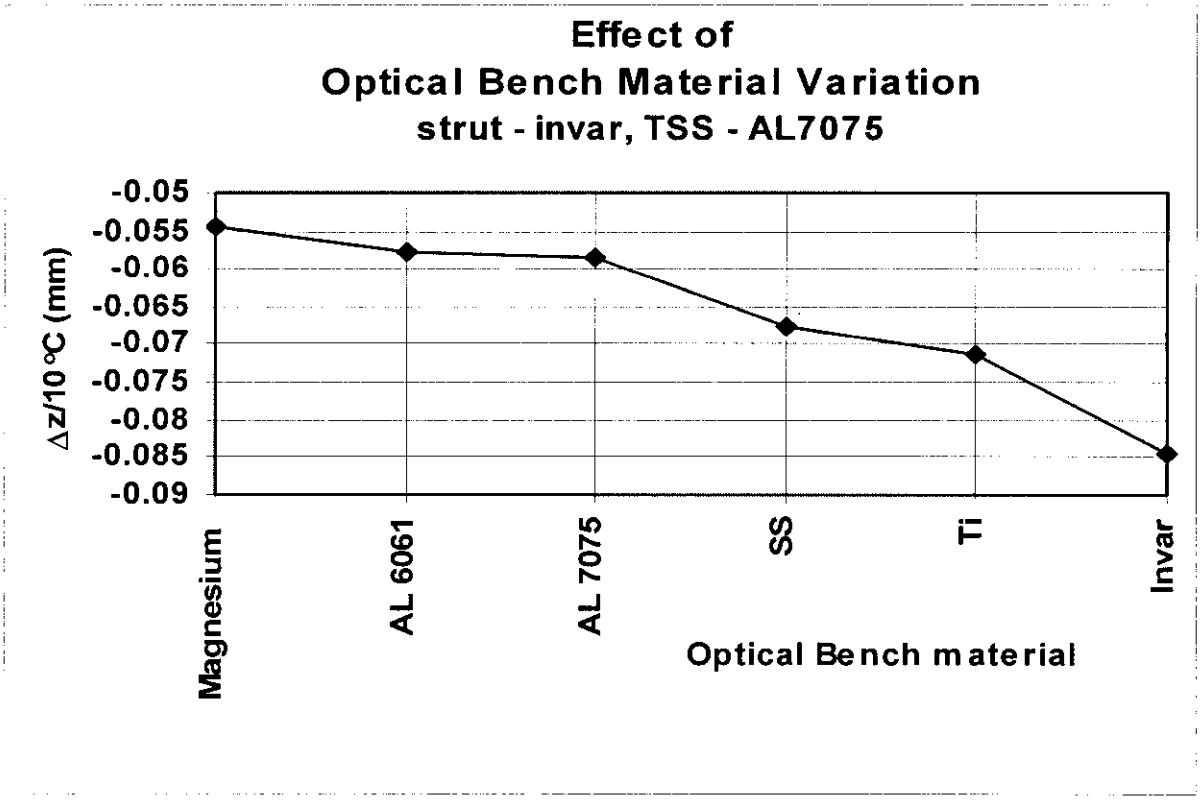

Figure 10 shows the focal distance, z, sensitivity to change in BFA optical bench material choice for a 10°C temperature change. Possible materials are shown in order of highest to lowest CTE. Figure 11 shows the focal distance, z, sensitivity to change in strut material choice for a 10°C temperature change. In addition, in Figure 11, a +/- variation in CTE value for each material is shown to demonstrate the possible performance of that material.

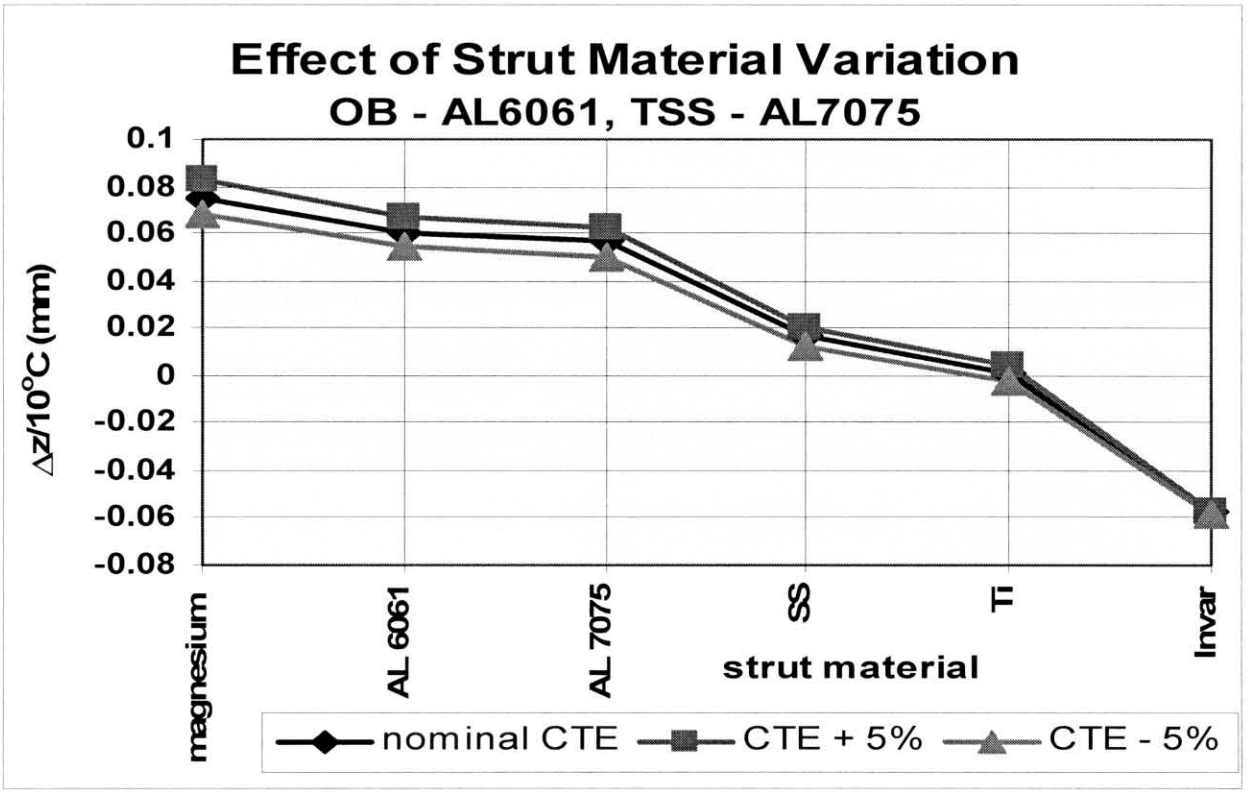

Figure 12. Change in z per 10°C versus variation in strut material

Summarizing, the process for determining the flight hardware choices was to impose predicted thermal gradients and average temperature variations, then use thermal and structural finite element models to calculate and compare final focal change performance for final design parameter selection. An additional variability was planned in the flight hardware design. Strut material options were increased by designing a two part strut as shown in Figure 13. This allowed an option for two materials with some shimming if necessary to "tune" in the required motion. The final analysis showed no need for this option so flight version ended up using Invar for both sides with no shims.

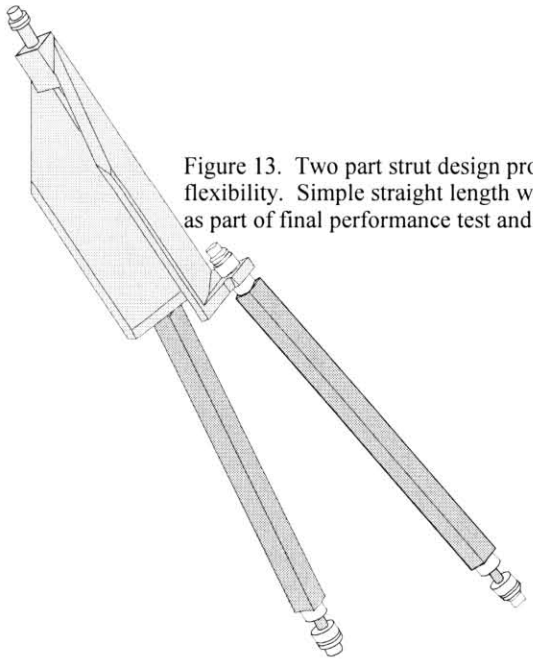

Figure 13. Two part strut design provided additional performance flexibility. Simple straight length was easy to machine and change as part of final performance test and assembly step.

5. FINAL FLIGHT DESIGN RESULTS

Final thermal analysis predicted thermal gradients through the TSP and BFA structures that varied during the telescope orbit around the sun between a hot case and cold case condition summarized in Table 3. A distribution of these

Table 3. Cold and hot case temperature conditions in orbit

Subassembly	Number	Cold Case (°C)	Hot Case (°C)
Telescope Support Structure	22	-9.3 to -10.0	8.0 to 9.1
Strut System	24	-7.0 to -3.2	11.8 to 15.7
Optical Bench	26-32	-0.1 to 4.2	18.8 to 24.0
NUV Detector	33	5.8	24.9
FUV Detector	34	3.9	22.3
M3	35	2.6	23
Dichroic	28	2.4	21.9

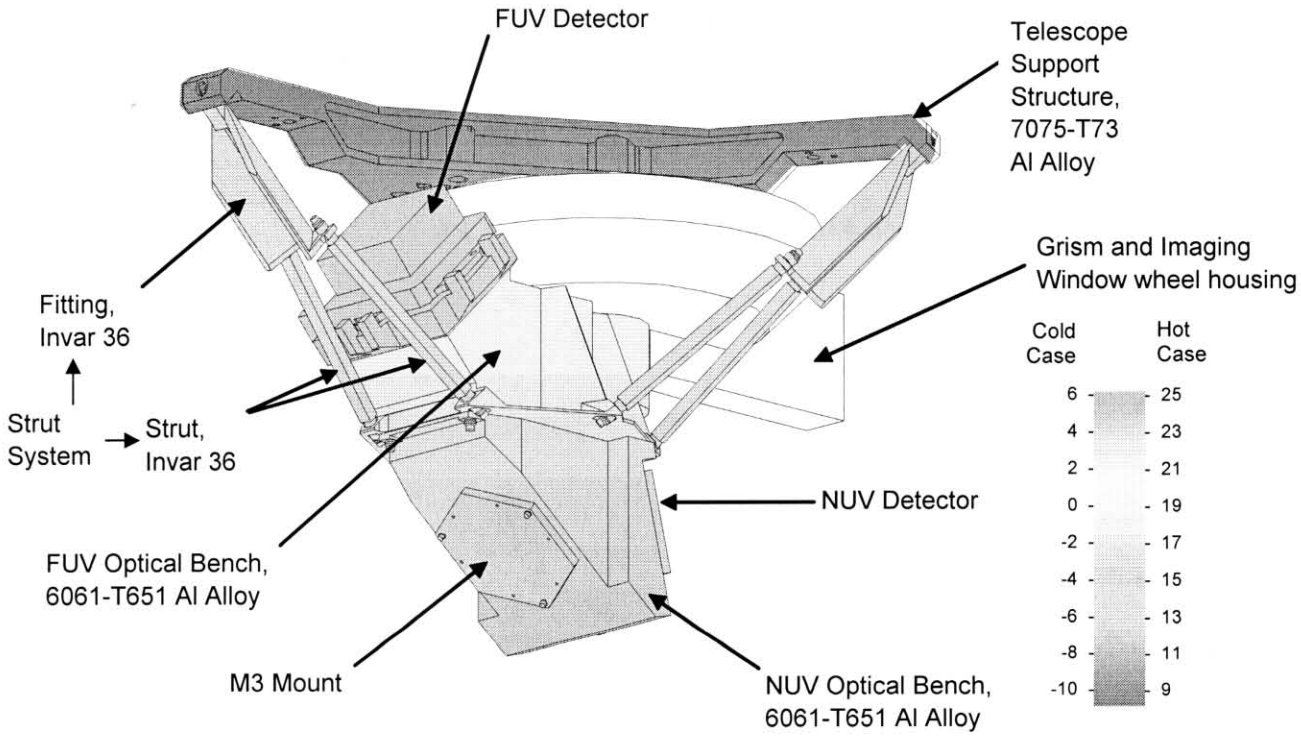

Figure 14. Thermal gradient conditions during flight

temperatures is shown in Figure 14. The system was tested on the ground recreating these temperature variations with measured performance results of the BFA thermal focus shift resulting in less than 10 microns of defocus from room temperature alignment throughout the range of expected thermal gradients. The allowable defocus budget for both the telescope and the BFA was 120 microns. Testing demonstrated that as long as the gradient distribution represented a constant difference in temperatures between components during the operational flight times, the system would perform to within the 10 micron defocus limit. The flight performance based on resulting images received demonstrates that this condition appears to be satisfied.

6. LESSONS LEARNED AND CONCLUSIONS

There were some limitations of this approach. It was difficult to find available volume to position symmetrical, equal-length bipods that avoided other hardware. All configuration choices aren't viable because of potential interferences. The final flight concept with the angle choices was a compromise that did allow bending stresses in the BFA optical bench structure. If the device being positioned were an optic, the bending stresses induced would have likely deformed the optic.

Another limitation was that Aluminum was the material of choice for both the Optical Bench and Telescope Support Structure. Materials options are often restricted by practical fabrication considerations.

In conclusion, though, this flexible athermalization design approach was able to accommodate and compromise to meet changing requirements. The images taken by GALEX since it launch, as shown in Figure 15, demonstrate the ability of this concept.

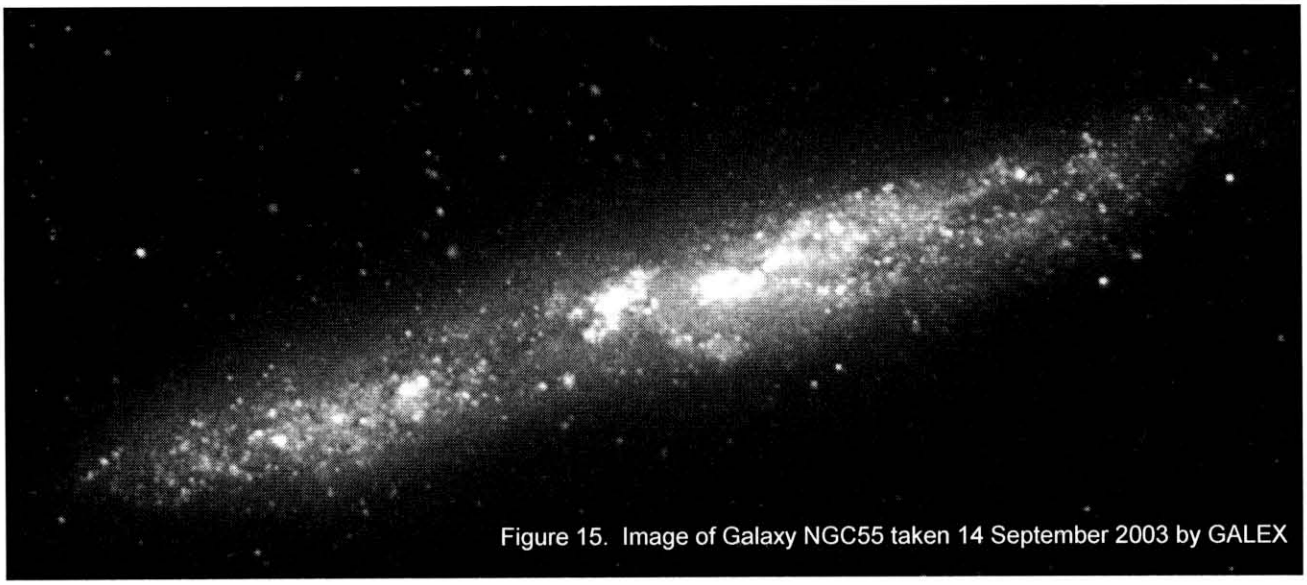

Figure 15. Image of Galaxy NGC55 taken 14 September 2003 by GALEX